



Paleoseismic Analysis of the Walanae Fault Zone in South Sulawesi, Indonesia

ASRI JAYA¹, OSAMU NISHIKAWA², and SAHABUDDIN JUMADIL¹

¹Department of Geological Engineering, Faculty of Engineering, Hasanuddin University, Makassar, Indonesia

²Department of Earth Resource Science, Faculty of International Resource Science, Akita University, Akita, Japan

Corresponding author: asri_jaya@geologist.com

Manuscript received: July, 8, 2021; revised: March, 14, 2022;

approved: April, 23, 2023; available online: August, 10, 2023

Abstract - The most seismogenic fault of South Sulawesi region is Walanae Fault, which has a moderate seismicity history with magnitudes ranging from Mw 4 to Mw 5. The largest earthquake occurred in 1997 with a magnitude of Mw 5.9. After the Donggala-Palu earthquake assailed Sulawesi Island in 2018, the fault in this region were reactivated, including the Walanae Fault system that has pair parallel faults, West Walanae Fault (WWF) and East Walanae Fault (EWF). This fault zone has a 150-km-long and 3-km-wide fault traces, and should have seismicity potential to produce larger earthquakes than the events measured to date. The resulting radiocarbon ages obtained from the dating of organic samples collected on two tranches along with the EWF support that the Walanae Fault zone has a longer earthquake history in the ranges of 4,000 BP (3,050 cal BP and 3,990 cal BP) and 100-300 AD (101 AD pMC and 340 cal BP). The results of age evidence suggest that the Walanae Fault system is an active fault, and must remain of concern as an earthquake source with potential hazards in the region, comprising the West Walanae Fault (WWF) and the East Walanae Fault (EWF). Both faults are separated by a narrow lowland area of Walanae Depression (25 km). The lowland area sandwiched by these two faults harboring a potential seismic amplification that might be generated by thick sediment filled the lowland.

Keywords: seismicity, earthquake, radiocarbon dating, Walanae Fault

© IJOG - 2023

How to cite this article:

Jaya, A., Nishikawa, O., and Jumadil, S., 2023. Paleoseismic Analysis of the Walanae Fault Zone in South Sulawesi, Indonesia. *Indonesian Journal on Geoscience*, 10 (2), p.215-227. DOI: [10.17014/ijog.10.2.215-227](https://doi.org/10.17014/ijog.10.2.215-227)

INTRODUCTION

Background

Sulawesi Island is located in a complex tectonic setting involving three large lithospheric plates: the Eurasian Plate to the west, Pacific Plate to the east, and Indian-Australian Plate to the south. Neogene tectonic history of Sulawesi is characterized by a continent-continent collision that occurred between Sundaland- and Australian Craton-derived blocks (Hamilton, W., 1979; Cofield *et al.*, 1993; Priadi *et al.*, 1994; Bergman *et al.*, 1996; Polvé *et al.*, 1997; Hall and Wilson, 2000; Hall, R., 2002; Jaya *et al.*, 2017) resulting in the development of large-scale active strike-slip faults, active thrust faults and extensions, and magmatism related to extensive lithospheric melting (Bergman *et al.*, 1996; Cipta *et al.*, 2017). Most large-scale active faults found in Sulawesi Island have potential to be earthquake sources. The crustal tectonic relation are Gorontalo strike-slip fault in the north arm of Sulawesi; Palu-Koro strike-slip fault and Poso thrust fault in the central of Sulawesi; Matano strike-slip fault, Balantak

al., 1996; Polvé *et al.*, 1997; Hall and Wilson, 2000; Hall, R., 2002; Jaya *et al.*, 2017) resulting in the development of large-scale active strike-slip faults, active thrust faults and extensions, and magmatism related to extensive lithospheric melting (Bergman *et al.*, 1996; Cipta *et al.*, 2017). Most large-scale active faults found in Sulawesi Island have potential to be earthquake sources. The crustal tectonic relation are Gorontalo strike-slip fault in the north arm of Sulawesi; Palu-Koro strike-slip fault and Poso thrust fault in the central of Sulawesi; Matano strike-slip fault, Balantak

Fault, Tolo thrust fault, and Batui thrust fault in the east arm of Sulawesi; Lawanopo and Kolaka strike-slip faults and Buton thrust Fault in the southeast arm of Sulawesi; and Makassar and Majene thrust faults, and Masupu, Walanae, Selayar strike-slip faults in the south arm of Sulawesi (Figure 1).

The variety of faults in this region is associated with intense seismic activities on individual faults, within the slab, and on the thrust faults. The structures of Sulawesi have moderate to high slip rates, and produce earthquakes with magnitudes of Mw 6-8 for individual faults and Mw > 8 for thrusts within the slab (Cipta *et al.*, 2017; PuSGeN, 2017). The MMI (Modified Mercalli Intensity) seismicity scale from V-IX is based on the 500-year return period, and almost all faults in the region have lowlands with accumulated

sediment that has a high amplification potential (Cipta *et al.*, 2017). Earthquake that occurred in 2018 with a Mw 7.2 magnitude, Donggala-Palu, followed by the Mw 6.2-magnitude Majene earthquake in 2021, proved that this region is prone to earthquakes; reflecting on the production of the two earthquakes, more severe damage occurred in lowland areas in the Palu and Mamuju Cities, even though the epicentres of the earthquakes were quite far (tens of km) from these two cities.

The Walanae Fault system is a major structure with prominent linear landform features that are traceable over 150 km through the southern arm of Sulawesi (Figure 1; Sukamto, 1975; van Leeuwen, 1981; Berry and Grady, 1987; van Leeuwen *et al.*, 2010; Jaya and Nishikawa, 2013; Cipta *et al.*, 2017). The system may even extend further into the Masupu Fault to the north in central Sulawesi.

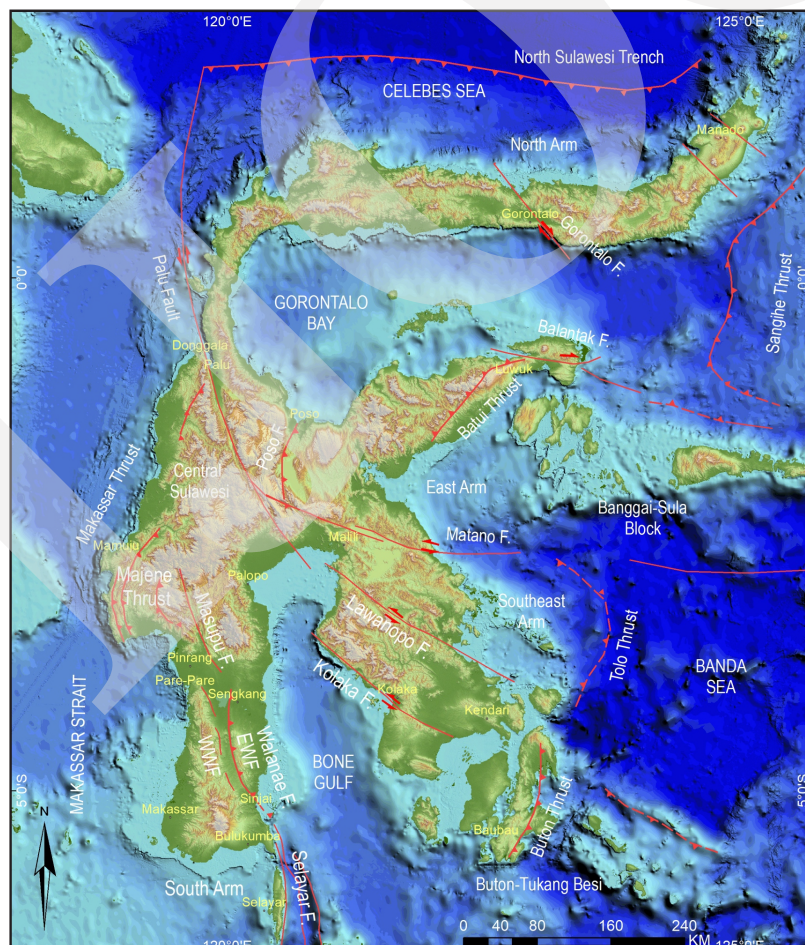


Figure 1. Topographic map and the main active fault structures of the Sulawesi region (modified after Sukamto 1975; Hall and Wilson, 2000; Watkinson, 2011; Cipta *et al.*, 2017; PuSGeN, 2017; Koesoemadinata, 2020; USGS; BMKG).

The Walanae Fault system comprises two parallel faults, West Walanae Fault (WWF) and East Walanae Fault (EWF), with a narrow topographic depression in between with younger accumulated sediments. The occurrence of a moderate earthquake with a Mw 5.9 magnitude was recorded in 1997, and the fact that this region has lowlands with soft sediments inhabited by the highest human population in Sulawesi Island causing the analysis of paleoseismicity and earthquake hazards in this region to be very important. Therefore, this study contributes new data for the evaluation of seismic hazards in the region.

Geological Settings

The geomorphic trace of the EWF can be recognized as a distinct topography between Bone Mountains and Walanae Depression, around which an intensive deformation zone is characterized by the development of faults, folds, and related structures at various scales (Guritno *et al.*, 1996; van Leeuwen *et al.*, 2010). Therefore, the EWF is thought to have played a major role in the structural and landform developments in this region during the Neogene. The predominance of a sinistral strike-slip motion in the EWF has been assumed based on the linear topographic features and the shear sense of its neighboring major faults, including Masupu Fault in the northern area (Coffield *et al.*, 1993; Guritno *et al.*, 1996; van Leeuwen *et al.*, 2010; Jaya and Nishikawa, 2013). Recently, the EWF was activated as a NE-SW-to-E-W-directed reverse fault with maximum compression since the Pliocene with a dextral slip component and pervasive development of secondary structures in the narrow zone between Bone Mountains and Walanae Depression (Jaya and Nishikawa, 2013).

It has been estimated that since the Early Miocene, the WWF Fault was involved in the formation of sedimentary rocks in Sengkang Basin. At a later stage, the EWF trace crossed the sedimentary rocks in Sengkang Basin, so it likely seems that the EWF is younger than the WWF Fault (van Leeuwen, 1981; Grainge and Davies, 1985; van Leeuwen *et al.*, 2010; Jaya

and Nishikawa, 2013). In the central area of the EWF, topography is more pronounced, and the Walanae Depression to the west and the high Bone Mountains to the east are separated by the EWF zone. The Walanae Depression is composed of a Middle Eocene to Late Pliocene stratigraphic succession consisting of marine sediments of Salokalupang Group, marine volcanic rocks of Bone Group, limestone of Taccipi Formation, and shallow marine to fluvio-deltaic sediments of the Walanae Formation (Figure 2). In the highlands of the Bone Mountains, bedrock is more purely composed of a succession of volcanic rocks, namely, potassic volcanic rocks of Late Miocene consisting of the Salokalupang Group and Bone Group (van Leeuwen *et al.*, 2010) or volcanic rocks of the Kalamiseng Formation (Sukanto, 1982). The northern edge of Bone Mountains forms the reef knolls of Tacipi Formation, which are thought to have grown in Late Middle-Late Miocene (Figure 2; Grainge and Davies, 1985; Ascaria *et al.*, 1997). Stratigraphic units are located in the fault zone between Bone Mountains and Walanae Depression and are involved in the deformation related to the EWF. Strata in this zone are sliced in variously sized fragments and tend to dip moderately to steeply eastward, running parallel approximately 3 km to the east. Several map-scale gentle folds occur, and their NE-SW to NNW-SSE trends are subparallel or slightly oblique to the general strike of EWF (van Leeuwen *et al.*, 2010; Jaya and Nishikawa 2013). These folds are covered by alluvial fan deposits provided via small rivers from Bone Mountains, and fan morphologies are scarcely distinct and are dissected by the channels.

In the northern part of studied area around Sengkang area, EWF has also been crossed by the EWF, causing the topography in the west to become lowlands and that in the east to form hills. The western lowlands, known as Walanae depression, where Lake Tempe is located, are generally filled with Quaternary sediments that are composed of lake deposits and river alluvial. While the hilly area to the east of the fault zone known as East Sengkang Basin has a sedimentary succession and comprises a series of Early

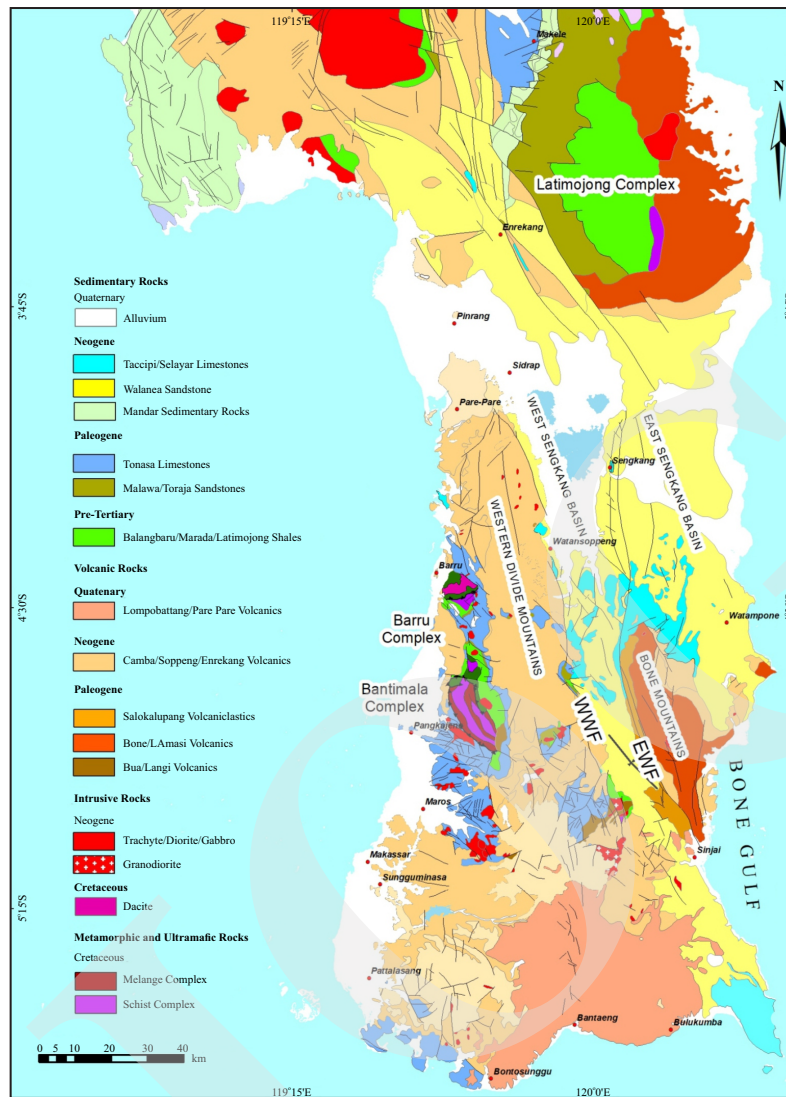


Figure 2. Geological map of the southern arm of Sulawesi (after Sukamto, 1975; Jaya and Nishikawa, 2013).

Miocene marine to shallow marine sediments (Mayall and Cox, 1988; van Leeuwen *et al.*, 2010). Locally, the upper part is also overlain by unconsolidated sediments (Figure 3). The western margin of the Senggang Basin comprises the EWF zone, forming a range of hills that are, structurally, a propagating fault tip forming the Senggang anticlinal hill.

METHODS AND MATERIALS

Radiocarbon dating was performed on four samples of organic matter included in the soil shear band, and this organic-rich soil horizon

was involved in deformation near the EWF trace. Sampling was carried out at two sites in the central and northern regions along the EWF scarps (Figure 3). The first location was exposed along a short cliff in the Lapaddata area around Bone Mountains, which is the central area of the fault trace. The area includes an alluvial fan derived from the EWF that is located approximately 1 km to the west of the main fault. Two sheared soil samples with label numbers ST-28A and ST-28B were collected in the wall of a quarry. The second location was along the Pattirosompe Hill around Senggang area on the northern part of the EWF line, located in the hills across the fault line on the east side of Senggang anticline. This region

comprises scarp-derived colluvium from the most recent event as a characteristic earthquake model (*e.g.* Schwartz and Coppersmith, 1984). The second collection of organic-rich soil samples with sample numbers SKM-02 and SKG-03 were collected in the wall of Pattirosompe quarry. The sample position was stratigraphically located beneath the crystalline carbonate outcrop of Taccipi Formation. All the samples were removed from weathered surfaces to prevent contamination.

The collected samples were sieved to separate root and plant debris, and then

treated with a hydrochloric acid (>3 N) wash to remove carbonate minerals from the organic matter. The samples were dated using accelerator mass spectrometry (AMS) at Beta Analytic Inc., Miami, Florida. The measured radiocarbon ages were converted to conventional radiocarbon ages (Stuiver and Polach, 1977), and calibrated by the IntCal04 calibration curve (Reimer *et al.*, 2004) and the SHCAL13 calibration curve (Hogg *et al.*, 2013). The $\delta^{13}C$ values were reported relative to PDB (Pee Dee Belemnite).

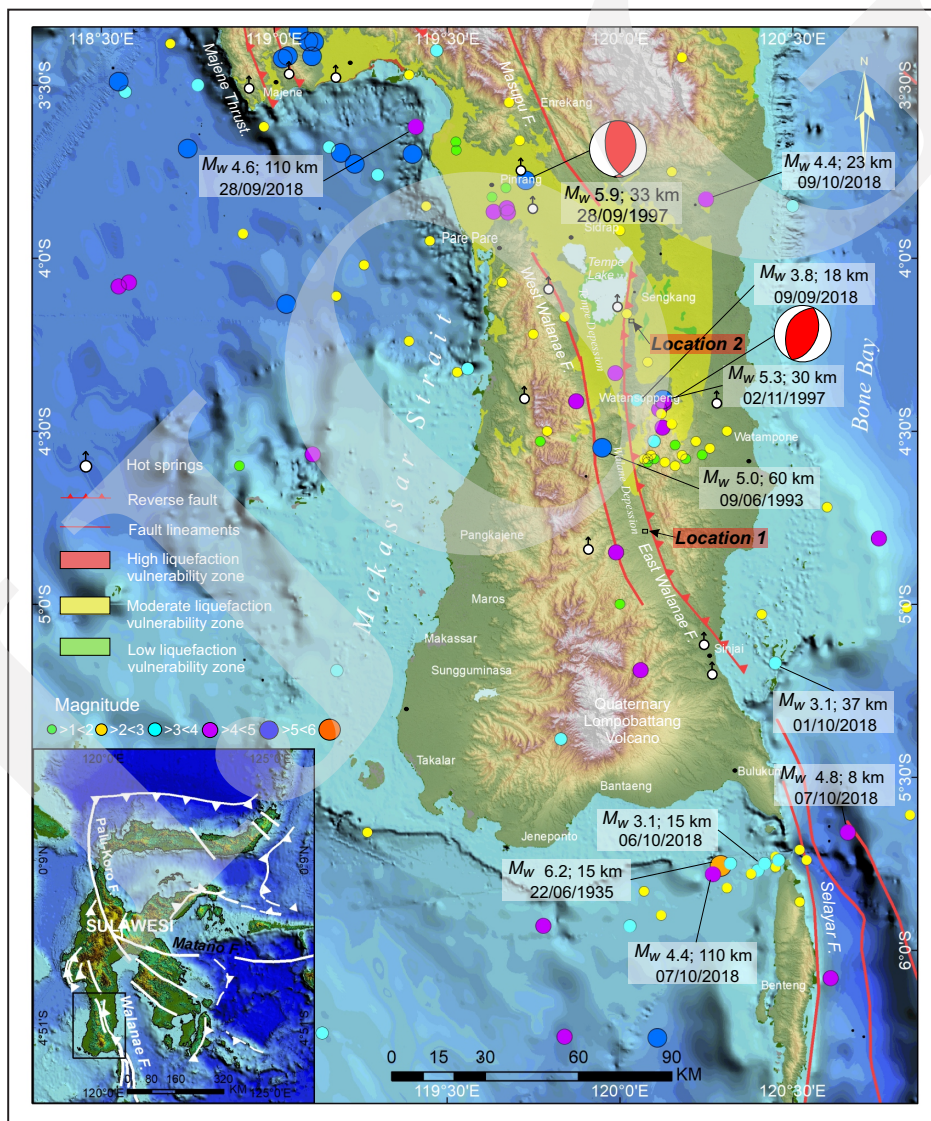


Figure 3. A topographic map was obtained from the DEM collected by a shuttle radar topography mission and a structural pattern map of the southern arm of Sulawesi (Jaya and Nishikawa, 2013). The distribution of epicenters from low to moderate events (Mw 2-6) and earthquake events that occurred from 1960-2019 around the Walanae region (Supartoyo and Suroso 2008; PuSGeN, 2017; Koesoemadinata, 2020; USGS; BMKG), the liquefaction vulnerability zones around Walanae region (Geological Agency of Indonesia, 2019), and each sample locality are also shown on the map.

RESULTS

Seismicity of the Walanae Fault

The earthquakes with low to moderate magnitudes ranging from Mw 4 to 5 lead to this region are rarely studied. A significant earthquake occurred in 1997 with a magnitude of Mw 5.9, at a depth of 33 km. This event damaged infrastructure in Pinrang City and the nearest urban area. To date, the slip rate is not yet known from GPS (PuSGeN, 2017). However, a strain rate of 3 mm/yr or less is suggested by GPS and seismological observations of the area covering the Makassar Block (Socquet *et al.*, 2006), which may include the EWF. However, the slip rate obtained from geological interpretations was recorded as 0.5 mm/yr (PuSGeN, 2017). Although their magnitudes were small, a series of earthquakes occurred after a large earthquake of Mw 7.5 in the northern Palu region on 28 September 2018: an earthquake of Mw 3.1 took place in Sinjai to the south of the EWF on 1 October 2018, and one of Mw 4.2 existed in to the north of the EWF on 9 October 2018 (Figure 3). A seismic hazard assessment of Sulawesi region indicated that Walanae Fault is classified as a high-intensity and moderate-hazard zone at 8 scales (MMI: V - VII) based on the 500-year return period and recurrence interval of 1.0 s (Cipta *et al.*, 2017).

The focal mechanism of seismic data obtained around the Walanae Fault trace is generally related to oblique and reverse faults, and it was illustrated that the current activity of the EWF is not only a strike-slip fault but also a reverse fault, especially in the onshore region and along the northern EWF trace. A similar indication is also strongly shown by paleostress data from a combination of fault-slip and calcite twin data, and evidence of sedimentary patterns suggests that the EWF was originally a strike-slip fault, and has now progressively become a reverse fault (Jaya and Nishikawa, 2013).

The latest seismicity surrounding location 1 has occurred around 1993-2018 with a range of Mw 2-5, the largest earthquake event was recorded to occur in the northwest in 1997 (Mw 5.9)

and the southeast (Mw 5.5). This area is mainly composed of carbonate and clastic sedimentary rocks of Walanae Formation which are covered by colluvium derived fault scarp from Walanae Fault (Figures 2 and 3). The latest seismicity surrounding location 2 has occurred in 1993-2018 with a range of Mw 2-5, the largest earthquake event recorded in the northwest in 1993 (Mw 5.0). This area mainly consists of Taccipi Formation that is cross-cut by the Walanae Fault (Figures 2 and 3).

Radiocarbon Dating of $\delta^{13}C$ Values

A sample representing the central area of the EWF was taken on the western foot of EWF scarps at the alluvial fan deposit sequence with intervening paleosols unconformably overlying the top of Salokalupang sequence (Figures 2 and 4). The samples used for radiocarbon dating were soils intercalated in the shear fractures formed in the weathered mudstone, which was intensely sliced by flexural slip folding that is most likely associated with the activity of the EWF (Figure 4d). The soils include dark-brown organic matter. Samples ST-28A and ST-28B, which were obtained 50 cm and 30 cm beneath the surface, respectively, yielded ages of 3,050 cal BP and 3,990 cal BP (Table 1). These radiocarbon ages were consistent with the stratigraphic order (Figures 4 and 5). The $\delta^{13}C$ (PDB) values of the dated soil samples are also shown in Table 1. Both samples show similar and significantly negative values, -18.4‰ for ST.28A and -19.6‰ for ST-28B (Table 1), which are plausible for grassland soils of grassland.

The samples representing the northern area of the EWF were taken on Sengkang anticline ridge. Two samples of organic-rich soil horizons obtained underneath the crystalline limestone of Walanae Formation at the same location of the Pattirosempe Hill in Sengkang area (Figures 2 and 6), not indirectly in stratigraphic order but still correlated in the field, were used for radiocarbon dating, as shown in Figures 6d and 6c. These soil samples came from a colluvial wedge on the eastern flank of The Sengkang anticline ridge. SKG-03 was collected 60 cm beneath the surface, while

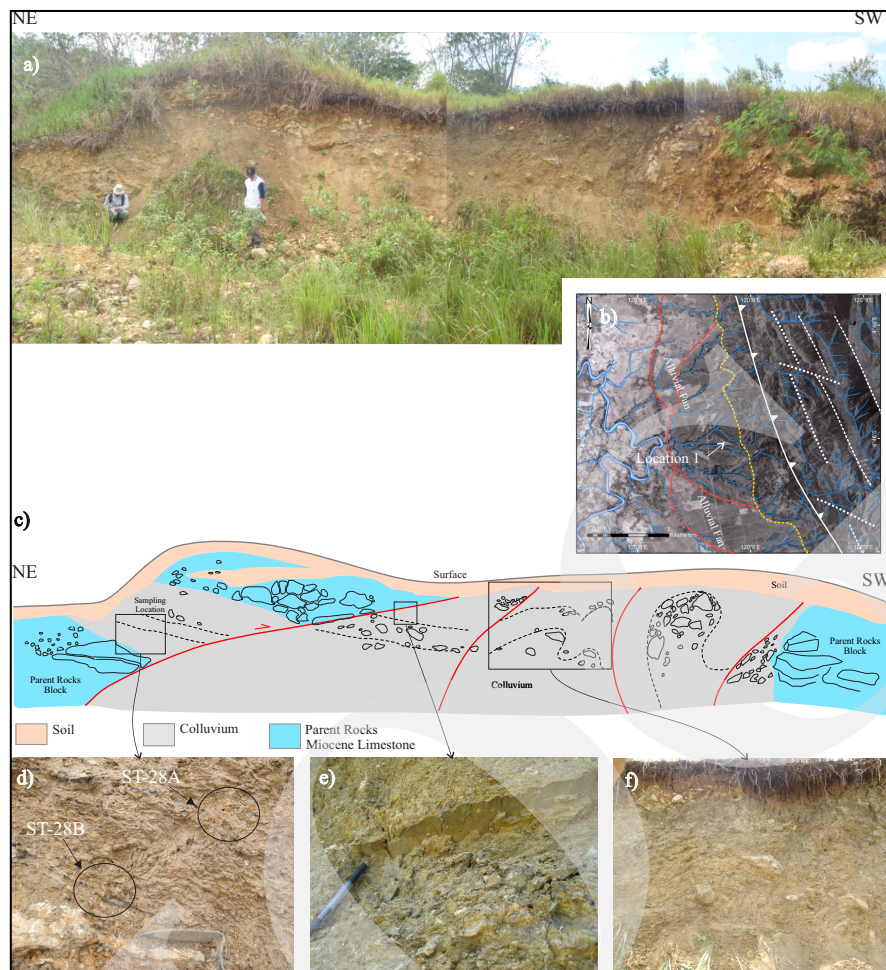


Figure 4. Photographs of: a) Outcrop exposure wall of mine quarry in location 1 of Bone area. b) Topographic map of the central part of the EWF showing the morphology and the structural situation around 1 of the Bone Mountains area. The EWF scarp-driven alluvial fans are on the western side and show the sample locality of the mining quarry. c) Sketches of exposure wall of the outcrop of Figure 5a showing stratigraphic order (soil, colluvium, parent rocks), and evidence of faulting, folding, sheared soils, and sample locality. d) Close-up of the occurrence of sheared soils that were sampled for radiocarbon dating at the east side of the outcrop (rectangle c); dark grey soils (arrows) are intercalated among the intensely sliced and weathered mudstone. e) Close-up of wall showing evidence of fault-slip cross-cut the colluvium layer (rectangle c). f) Close-up of wall showing the beds of mudstones are intensely sheared and the limestones are fragmented (rectangle c).

Table 1. Radiocarbon Age Dating of Soil Samples

Locality	Sample number	Lab sample number ^(a)	Measured radiocarbon age	$\delta^{13}C(\text{‰})$	Conventional radiocarbon age (BP) ^(b)	Calibrated age 2σ
Location 1: Central Area	ST-28A	Beta-286412	2940 ± 40	-18,4	3050 ± 40	Cal BC 1410-1210, Cal BP 3360-3160 (95% probability) ^(c)
	ST-28B	Beta-286413	3900 ± 40	-19,6	3990 ± 40	Cal BC 2580-2460, Cal BP 3530-4410 (95% probability) ^(c)
Location 2: Northern Area	SKM-02	Beta-437032	101 ± 40	-24,6	101 ± 50	pMC = percent modern carbon
	SKG-03	Beta-479286	340 ± 30	-19,6	340 ± 30	Cal AD 1496 - 1650, 454 - 300 cal BP (95.4% probability) ^(d)

(a) Processing and measurement of samples were carryout at Beta Analytic Inc. Miami, Florida.

(b) Conventional ^{14}C ages were calculated according to Stuiver and Polach, 1977.

(c) Calibration of radiocarbon age to calendar years was performed using "IntCal04" (calibration of radiocarbon, volume 46, 2004).

(d) Calibration of radiocarbon age to calendar years was performed using "SHCAL13" (calibration issue of radiocarbon, volume 55, 2013).

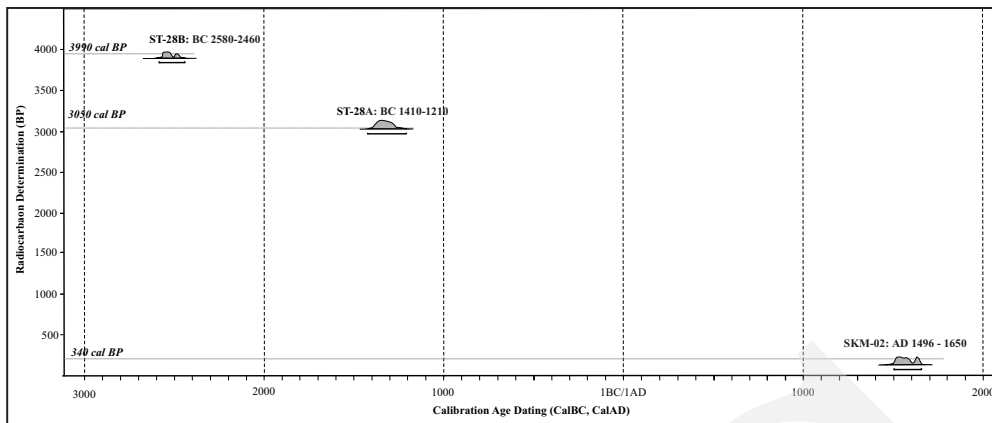


Figure 5. A calibration diagram and age distribution of radiocarbon dates of Walanae Fault. Calibrations were obtained using IntCal04 curve (Reimer *et al.*, 2004) and “SHCAL13” curve (Hogg *et al.*, 2013).

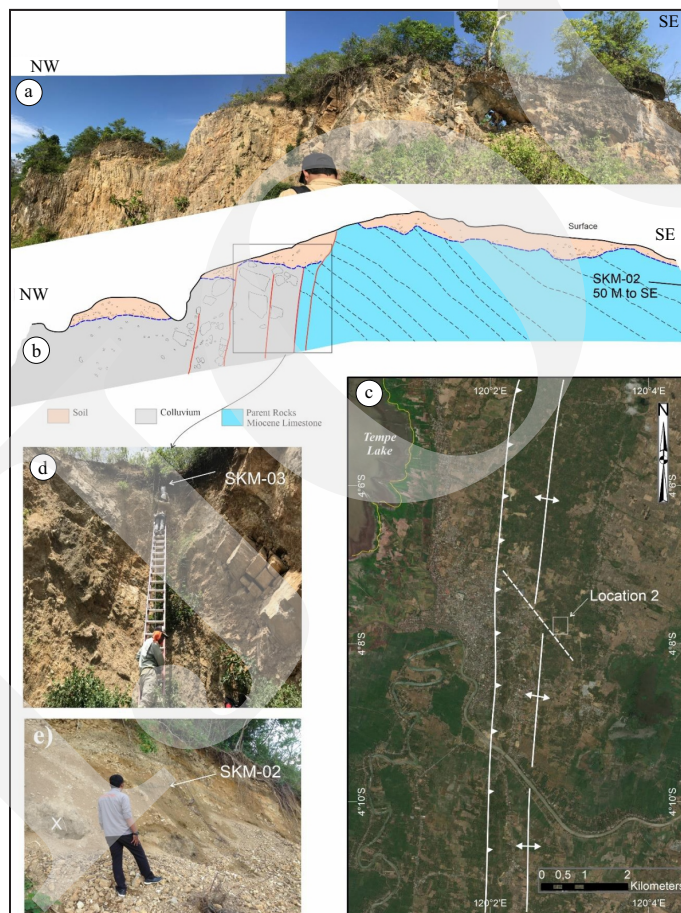


Figure 6. a) The exposure wall of crystalline carbonate outcrops in the mining quarry in location 2 of the Sengkang area. b) Sketches of exposure wall of the outcrop of figure 6a showing stratigraphic order (soil, colluvium, parent rocks), and evidence of fault scarp, layer rocks, and sample locality. c) Topographic map and structural components of the central part of the EWF showing the morphology and structural situation around location 2 of the Sengkang area. d) Close-up of the occurrence of the organic-rich horizons that were sampled for radiocarbon dating of SKG-03 (rectangle b). e) Site of SKM-02 soil sampling (arrow); the “X” marking is the continuity of the horizon of SKG-03.

SKM-02 was collected 100 cm from the surface. Stratigraphically, SKG-03 was older than SKM-02 (Figures 6d and 6e). The dating results were

also consistent with the stratigraphic order (Table 1); SKM-02 yielded an age of 101 AD pMC, and SKG-03 yielded an age of 340 cal BP. This ~200-

year difference represents two different earthquake events. The $\delta^{13}\text{C}$ (PDB) values of the dated soil samples (Table 1) both show similar and significantly negative values, -24.6 ‰ for SKM-02 and -19.6 ‰ for SKG-03 (Table 1; Figure 5), which are also plausible for grassland soils.

Compared to location 2 in the northern area of the EWF, the age at location 2 in Sengkang area represents the most recent faulting event at this site. The gap of ~2,700 to ~2,900 years in both locations shown in Table 1 is likely because the sample at location 1 is a fissure and crack of the alluvial fan located far away from the main fault, approximately ± 1 km from the EWF scarps (Figure 6b). Whereas the sample obtained from location 2 represents a direct deposition wedge from the Walanae Fault trace. All organic soil data have revealed a good paleoseismic record around the region. To assess seismic risk in the future, more information is still needed to add to the comprehensive study of this area.

DISCUSSION

Paleoseismicity of Walanae Fault

Although no obvious tectonic landform has been found and the current seismicity around the EWF seems relatively low compared to that in Central and North Sulawesi (Socquet *et al.*, 2006; Bellier *et al.*, 2006; Tanioka and Yudhicara, 2008; Jaya *et al.*, 2019), Late Quaternary deformation associated with EWF activity is confirmed by our radiocarbon dating results, yielding deformation periods of approximately BC ~3,000 to ~4,000 and AD ~100 to ~300 (Table 1; Figure 4). Based on seismotectonic studies, the present-day deformation and stress field in South Sulawesi are characterized by a compressional regime with ESE-WNW (N99°E)-trending σ_1 , showing the dominance of reverse faulting in South Sulawesi (Beaudouin *et al.*, 2003; Tanioka and Yudhicara, 2008; Jaya and Nishikawa, 2013). Therefore, it can be accepted that the stress states of the E-W to NE-SW general compression have continued consistently since Late Miocene.

Currently, no data are available on the average rupture length or slip rate of Walanae Fault. However, if empirical relationships are applied (*e.g.* Wells and Coppersmith, 1994), when the entire fault (~150 km) ruptures at once, by applying the modern-magnitude earthquakes with average magnitudes of Mw 5-6 that did not rupture the surface in these areas, with such a rupture length, the fault is likely to produce an earthquake with a magnitude of Mw 6-7. This magnitude seems to agree with the rupture scenarios of future events.

Earthquake Hazard of Walanae Fault

Individual earthquake hazards along the Walanae Fault trace appear to be high, with the lowlands along with the Walanae Depression and Tempe Depression created by the fault leading to high ground motion amplification (at site classes D and E) (Cipta *et al.*, 2017). Part of the depression area was classified as a moderate liquefaction-vulnerability zone (Geological Agency of Indonesia, 2019). The earthquake history was recorded from 1993 to 1997 in the northern part of Walanae Valley with an average magnitude of Mw 4-5; an earthquake occurred in 1997 with a magnitude of Mw 5.9 in the same area (Figure 2). The earthquake was recorded to have caused the deaths of sixteen people and destroyed hundreds of buildings (local government and online news information). These high-potential earthquake hazards and paleoseismicity have been correlated well with the historical damaging earthquakes in the region, except for the damaging 29/12/1828 earthquake in Bulukumba, which had an MMI scale of VIII-IX, earthquakes that have occurred on the south coast of South Sulawesi, and even the tsunami that occurred around Makassar in 1820 with MMI scale VII (Supartoyo and Surono, 2008). However, monitoring of the earthquakes that occurred ± 200 years ago was not equipped with coordinated information, and it is possible that these earthquakes were caused by either The Walanae Fault or an unmapped offshore extension of this structure to the SE (Cipta *et al.*, 2017).

However, in general, fewer historical earthquakes have been recorded in this region com-

pared with those recorded over the entire island. Research and documentation of earthquake hazard data in this region should be continued since the region contains several small towns inhabited by significant populations, with an average of 50,000 inhabitants in towns in Walanae Valley from north to south, such as Pinrang, Pangkajene-Sidrap, Sengkang, Sinjai, and Bulukumba. It can also be considered that the major faults in the middle part of Sulawesi are quite large in intensity and magnitude. Thus, if ground shaking occurs due to a large earthquake in this area, it may be influenced by Walanae region, such as Palu earthquake of 2018. Another consideration is that physiographically, this region is the boundary between Walanae Valley and the northern highlands of Majene and Masupu Faults, which can be influenced by these thrust faults with high earthquake intensities and seismicity. When a major earthquake occurred in Central Sulawesi in 2018, this region also showed a significant activity.

CONCLUSIONS

The novel insights derived from the field investigations, radiocarbon dating, paleoseismic analysis, and earthquake hazard analysis of the Walanae Fault in the southern arm of Sulawesi can be summarized in the following points.

- The Late Quaternary radiocarbon ages of BC 3,050 cal BP and 3,990 cal BP obtained for the sheared soils were collected from the western fault scarp of East Walanae Fault in Bone area (location 1) indicated two earthquake events and suggested present-day deformation around East Walanae Fault.
- The most recent two radiocarbon ages obtained via dating of organic-rich soils (101 AD pMC and 340 cal BP) were measured in the scarp-derived colluvium of main faults of East Walanae Fault in Sengkang area (location 2), confirming paleo-seismic EWF activity.
- The significant recent earthquake that occurred in 1997 around Walanae Depression showed

that both Walanae Fault and the lowlands have high future potential earthquake hazards.

ACKNOWLEDGEMENTS

This research was funded by The International Research Collaboration (PKLN 2018) and Fundamental Research (PDU 2020) of Hasanuddin University. The authors express gratitude and appreciation to The Ministry of Education and Culture of Indonesia and Hasanuddin University for providing a research grant. The authors thank the reviewers for helpful comments and advice. Finally, thanks go to the students of Hasanuddin University for supporting the authors during the field survey.

REFERENCES

- Ascaria, N.A., Harbury, N.A., and Wilson, M.E.J., 1997. Hydrocarbon potential and development of Miocene knoll-reefs, South Sulawesi. *Proceedings of the Petroleum Systems of SE Asia and Australasia Conference*, May 1997, p.569-584. DOI: 10.29118/ipa.2277.569.584
- Beaudouin, T.H., Bellier, O., and Sebrier, M., 2003. Present-day stress and deformation field within the Sulawesi Island area (Indonesia): geodynamic implications. *Bulletin de la Société géologique de France*, 174, p.305-317. DOI: 10.2113/174.3.305
- Bellier, O., Sebrier, M., Seward, D., Beaudouin, T., Villeneuve, M., and Putranto, E., 2006. Fission track and fault kinematics analyses for new insight into the Late Cenozoic tectonic regime changes in West-Central Sulawesi (Indonesia). *Tectonophysics*, 413, p.201-220. DOI: 10.1016/j.tecto.2005.10.036
- Bergman, S.C., Coffield, D.Q., Talbot, J.P., and Garrard, R.J., 1996. Tertiary tectonic and magmatic evolution of western Sulawesi and the Makassar Strait, Indonesia. Evidence for a Miocene continent-continent collision. *In:*

- Hall, R. and Blundell, D.J. (eds), *Tectonic Evolution of SE Asia*, Geological Society of London, *Special Publications*, 106, p.391-430. DOI: 10.1144/gsl.sp.1996.106.01.25
- Berry, R.F. and Grady, A.E., 1987. Mesoscopic structures produced by Plio-Pleistocene wrench faulting in South Sulawesi, Indonesia. *Journal of Structural Geology*, 9, p.563-571. DOI: 10.1016/0191-8141(87)90141-6
- BMKG (Meteorological, Climatological and Geophysical Agency of Indonesia). <https://www.bmkg.go.id/?lang=EN>.
- Cipta, A., Robiana. R., Griffin, J.D., Horspool, N., Hidayati, S., and Cummings, P.R., 2017. A probabilistic seismic hazard assessment for Sulawesi, Indonesia. In: Cummins, P.R, Meilano, I. (eds), *Geohazards in Indonesia: earth science for disaster risk reduction. Geological Society Special Publications*, 44, p.133-152. DOI: 10.1144/sp441.6
- Coffield, D.Q., Bergman, S.C., Carrard, R.A., Guritno, N., Robinson N.M., and Talbot, J., 1993. Tectonic and stratigraphic evolution of the Kalosi PCS area and associated development of a Tertiary petroleum system, South Sulawesi, Indonesia. *Proceedings of the Indonesian Petroleum Association*, 22 (1), p.679-706. DOI: 10.29118/ipa.2500.679.706
- Geological Agency of Indonesia, 2019. *Atlas of liquefaction vulnerability zone of Indonesia*. Ministry of Energy and Mineral Resources of Indonesia-Centre of Groundwater Resources and Environmental Geology.
- Grainge, A.M. and Davies, K.G., 1985. Reef exploration in the East Sengkang Basin, Sulawesi, Indonesia. *Marine and Petroleum Geology*, 2, p142-155. DOI: 10.1016/0264-8172(85)90004-2
- Guritno, N., Coffield, D.Q., and Cook, R.A., 1996. Structural development of Central South Sulawesi. *Proceedings of the Indonesian Petroleum Association*, 25, p.253-266.
- Hall, R. and Wilson, M.E.J., 2000. Neogene sutures in eastern Indonesia. *Journal of Asian Earth Sciences*, 18, p.781-808. DOI: 10.1016/S1367-9120(00)00040-7
- Hall, R., 2002. Cenozoic geological and plate tectonic evolution of SE Asia and the SW Pacific: computer-based reconstructions, model and animations. *Journal of Asian Earth Sciences*, 20, p.235-431. DOI: 10.1016/S1367-9120(01)00069-4
- Hamilton, W., 1979. *Tectonics of the Indonesian region*. U.S. Geological Survey Professional Paper 1078.
- Hogg, A.G., Hua, Q., Blackwell, P.G., Niu, M., Buck, C.E., Guilderson, T.P., Heaton, T.J., Palmer, J.G., Reimer, P.J., Reimer, R.W., Turney, C.S.M., and Zimmerman, S.H.R., 2013. SHCAL13 Southern Hemisphere Calibration, 0-50,000 Years Cal BP. *Radiocarbon*, 55 (4), p 1889-1903. 10.2458/azu_js_rc.55.16783
- Jaya, A. and Nishikawa, O., 2013. Paleostress reconstruction from calcite twin and fault-slip data using the multiple inverse method in the East Walanae fault zone: Implications for the Neogene contraction in South Sulawesi, Indonesia, *Journal of Structural Geology*, 55, p.34-49. DOI: 10.1016/j.jsg.2013.07.006
- Jaya, A., Nishikawa, and O., Hayasaka, Y., 2017. LA-ICP-MS Zircon U-Pb and Muscovite K-Ar Ages of Basement Rocks from the South Arm of Sulawesi, Indonesia. *Lithos*, 291293, p.96-110. DOI: 10.1016/j.lithos.2017.08.023
- Jaya, A., Nishikawa, and O., Jumadil, S., 2019. Distribution and morphology of the surface ruptures of the 2018 Donggala-Palu earthquake, Central Sulawesi, Indonesia. *Earth Planets and Space*, 71/144, p.1-13. DOI: 10.1186/s40623-019-1126-3
- Jaya, A., Nishikawa, and O., Jumadil, S., 2021. Fluid migration along faults and gypsum vein formation during basin inversion: An example in the East Walanae fault zone of the Sengkang Basin, South Sulawesi, Indonesia. *Marine and Petroleum Geology*, 133, 105308. DOI: 10.1016/j.marpetgeo.2021.105308
- Koesoemadinata, R.P., 2020. *An Introduction into The Geology of Indonesia*. Ikatan Alumni Geologi, Institut Teknologi Bandung, 2, 200pp.
- Mayall, M.J., Cox, M., 1988. Deposition and diagenesis of Miocene limestones, Sengkang

- Basin, Sulawesi, Indonesia. *Sedimentary Geology*, 59, p.77-92 DOI: 10.1016/0037-0738(88)90100-5
- Polvé, M., Maury, R.C., Bellon, H., Rangin, C., Priadi, B., Yuwono, S., Joron, J.L., and Soeria-Atmadja, R., 1997. Magmatic evolution of Sulawesi: constraints on the Cenozoic geodynamic history of the Sundaland active margin. *Tectonophysics*, 272, p.69-92. DOI: 10.1016/s0040-1951(96)00276-4
- Priadi, B., Polvé, M., Maury, R.G., Bellon, H., Soeria-Atmadja, R., Joron, J.L., and Cotton, J., 1994. Tertiary and Quaternary magmatism in Central Sulawesi: chronological and petrological constraints. *Journal of Southeast Asian Earth Sciences*, 9 (1-2), p.81-93. DOI: 10.1016/0743-9547(94)90067-1
- PuSGeN (National Centre for Earthquake Studies), 2017. *Seismic Source and Hazard Map of Indonesia*. <http://litbang.pu.go.id/puskim/berita/detail/1355/peta-sumber-dan-bahaya-gempa-indonesia-tahun-2017>.
- Reimer, P.J., Baillie, M.G.L., Bard, E., Bayliss, A., Beck, J.W., Bertrand, C.J., Blackwell, P.G., Buck, C., Burr, G.S., Cutler, K.B., Damon, P.E., Edwards, R.L., Fairbanks, R.G., Friedrich, M., Guilderson, T.P., Hogg, A.G., Hughen, K.A., Kromer, B., McCormac, G., Manning, S., Ramsey, C.B., Reimer, R.W., Remmele, S., Southon, J.R., Stuiver, M., Talamo, S., Taylor, F.W., van der Plicht, J., and Weyhenmeyer, C.E., 2004. IntCal04 terrestrial radiocarbon age calibration, 0-26 cal kyr BP. *Radiocarbon*, 46, p.1029-1058. DOI: 10.1017/s0033822200033002
- Schwartz, D.P. and Coppersmith, K.J., 1984. Fault behavior and characteristic earthquakes: Examples from the Wasatch and San Andreas Fault zones. *Journal of Geophysical Research: Solid Earth*, 89 (B7), p.5681-5698. DOI: 10.1029/jb089ib07p05681
- Socquet, A., Vigny, C., Chamot-Rooke, N., Simons, W., Rangin, C., and Ambrosius, B., 2006. India and Sunda plate motion and deformation along their boundary in Myanmar determined by GPS. *Journal of Geophysical Research*, 111, p.1-15. DOI: 10.1029/2005JB003877.
- Stuiver, M. and Polach, H.A., 1977. Discussion reporting of ^{14}C data. *Radiocarbon*, 19, p.355-363. DOI: 10.1017/s0033822200003672
- Sukanto, R., 1975. The structure of Sulawesi in the light of plate tectonics. Paper presented at *The Regional Conference on the Geology and Mineral Resources of SE Asia, Jakarta*, p.1-25.
- Sukanto, R., 1982. *Geologi Lembar Pankajene dan Watampone Bagian Barat, Sulawesi*. Geological Research and Development Centre, Bandung.
- Supartoyo and Surono, 2008. *Catalog of Indonesian Destructive Earthquake, the Year 1629-2007*. Badan Geologi (Geological Agency of Indonesia), Jawa Barat.
- Tanioka, Y. and Yudhicara., 2008. Teleseismic body wave data analysis for the May 4, 2000, Sulawesi Earthquake. *Jurnal Geoplrika*, 3 (2), p.071-080.
- USGS (United States Geological Survey), 2020 <https://earthquake.usgs.gov/earthquakes/search/>
- Van Leeuwen, T.M., 1981. The geology of southwest Sulawesi with special reference to the Biru area. In: Barber, A. and Wiryosujono, S. (eds.), *The Geology and Tectonics of Eastern Indonesia*, Geological Research and Development Centre, *Special Publication*, 2, p.277-304.
- Van Leeuwen, T.M., Susanto, E.S., Maryanto, S., Hadiwisastra, S., Sudijono, and Muharjo., 2010. Tectonostratigraphic evolution of Cenozoic marginal basin and continental margin successions in the Bone Mountains, South Sulawesi, Indonesia. *Journal of Asian Earth Sciences*, 38, p.233-254. DOI: 10.1016/j.jseaes.2009.11.005
- Watkinson, I.M., 2011. Ductile in the metamorphic rocks of central Sulawesi. In: Hall, R., Cottam, M.A., Wilson, M.E.J. (eds.), *The SE Asian Gateway: History and Tectonics of the Australia-Asia Collision*, Geological Society of London, *Special Publications*, 355, p.157-176. DOI: 10.1144/sp355.1

Wells, D.L. and Coppersmith, K.J., 1994. Empirical relationships among magnitude, rupture length, rupture width, rupture area, and surface

displacement. *Bulletin Seismological Society of America*, 84 (4), p.974-1002

UJOG